

Magneto-optics of bilayer graphene inclusions in rotational-stacked multilayer epitaxial graphene

M. Orlita,^{1,2,*} C. Faugeras,¹ J. Borysiuk,³ J. M. Baranowski,⁴ W. Strupiński,⁵ M. Sprinkle,⁶ C. Berger,^{6,7} W. A. de Heer,⁶ D. M. Basko,⁸ G. Martinez,¹ and M. Potemski¹

¹Laboratoire National des Champs Magnétiques Intenses,
CNRS-UJF-UPS-INSA, 25, avenue des Martyrs, 38042 Grenoble, France

²Institute of Physics, Faculty of Mathematics and Physics,
Charles University, Ke Karlovu 5, 121 16 Praha 2, Czech Republic

³Institute of Physics, Polish Academy of Sciences, 02-668 Warsaw, Al. Lotnikow 32/46, Poland

⁴Institute of Experimental Physics, University of Warsaw, Hoza 69, PL 00-681 Warsaw, Poland

⁵Institute of Electronic Materials Technology, PL 01-919 Warsaw, Poland

⁶School of Physics, Georgia Institute of Technology, Atlanta, Georgia 30332, USA

⁷Institut Néel/CNRS-UJF BP 166, F-38042 Grenoble Cedex 9, France

⁸Laboratoire de Physique et Modélisation des Milieux Condensés, UJF and CNRS, F-38042 Grenoble, France

(Dated: November 5, 2018)

Additional component in multi-layer epitaxial graphene grown on the C-terminated surface of SiC, which exhibits the characteristic electronic properties of a AB-stacked graphene bilayer, is identified in magneto-optical response of this material. We show that these inclusions represent a well-defined platform for accurate magneto-spectroscopy of unperturbed graphene bilayers.

PACS numbers: 71.55.Gs, 76.40.+b, 71.70.Di, 78.20.Ls

I. INTRODUCTION

The absence of the energetic gap in the excitation spectrum of graphene¹ is considered as a possible drawback preventing the straightforward application of this emerging material in electronics. This is despite numerous efforts, such as those implying surface patterning² and substrate- or adsorbents-induced interactions.³⁻⁵ The possibility to open and tune the band gap in the bilayer graphene has recently been demonstrated by applying an electric field perpendicular to the graphitic planes⁶⁻⁸ and this is a key element to construct a transistor, the building block of electronic circuits. The band gap engineering is “typical” of the bilayer and is not reported in tri- and more-layer graphene specimens where semi-metallic behavior dominates.⁹ From the viewpoint of applications, the bilayer graphene thus becomes almost equally appealing material as graphene itself.

Optical spectroscopy has played an important role in investigations of the bilayer graphene,^{6,10,11} as, for instance, it allows to directly visualize the electric-field induced energy gap in this system.^{7,8} On the other hand, only relatively scarce information has been up to now collected from *magneto*-optical measurements.¹² This fact might be surprising when noticing the potential of Landau level (LL) spectroscopy which has been widely applied to other graphene-like systems. Magneto-optical methods have, for example, convincingly illustrated the unconventional LL spectrum in graphene, have offered a reliable estimate of the Fermi velocity or invoked the specific effects of many-body interactions between massless Dirac fermions.¹³⁻¹⁹

So far, the only magneto-optical experiments on the bilayer graphene have been reported by Henriksen *et al.*,¹² who succeeded to probe a relatively weak cyclotron-

resonance signal of a small flake using the gate-controlled differential technique. The optical response at a fixed magnetic field was then studied as a function of the carrier density. Such differential spectroscopy was efficient in case of exfoliated graphene monolayers,^{14,18} but it provides more complex results when applied to the bilayer graphene. In this latter system, the change of the gate voltage affects not only the carrier density but also modifies significantly the band structure and data interpretation is by far more elaborated.²⁰

In this paper, we demonstrate that certain class of previously reported AB-stacking faults²¹⁻²⁴ in otherwise rotationally-ordered multilayer epitaxial graphene (MEG),^{13,25-27} show the characteristic features of well-defined graphene bilayers. These inclusions, identified here in magneto-transmission experiments, represent therefore a suitable system for accurate magneto-spectroscopy studies of unperturbed bilayer graphene.

II. SAMPLE PREPARATION AND EXPERIMENTAL DETAILS

The growth of MEG samples studied here was performed with a commercially available horizontal chemical vapor deposition hot-wall reactor (Epigress V508), inductively heated by a RF generator. Epitaxial MEG films were grown on semi-insulating 4H-SiC(000 $\bar{1}$) on-axis C-terminated substrates at 1600°C in Ar atmosphere. The growth rate was controlled by the Ar pressure (~ 100 mbar) which was found to directly influence the evaporation rate of Si atoms.

To measure the infrared transmittance of our samples, we used the radiation of a globar, which was analyzed by a Fourier transform spectrometer and delivered to the

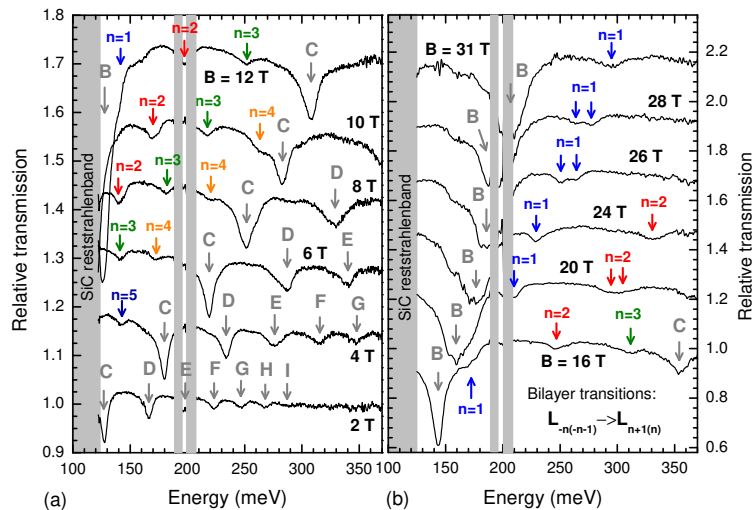


FIG. 1: (color online) Transmission spectra of MEG with ~ 100 layers recorded at the selected magnetic fields below 12 and above 16 T in parts (a) and (b), respectively, in both cases above the reststrahlenband of SiC. Whereas the transitions marked B to I correspond to electrically isolated graphene monolayers, transitions denoted $n = 1$ to 5 match to inter-LL transitions in an unperturbed graphene bilayer, following the coding $L_{-n(-n-1)} \rightarrow L_{n+1(n)}$. For clarity, successive spectra in parts (a) and (b) are shifted vertically by 0.14 and 0.23, respectively.

sample via light-pipe optics. The transmitted light was detected by a composite bolometer kept at $T = 2$ K and placed directly below the sample. Measurements were carried out in superconducting ($B = 0 - 13$ T) and resistive ($B = 13 - 32$ T) solenoids with spectral resolution of 0.5 and 1 meV in the range of magnetic field below and above $B = 13$ T, respectively. All presented spectra were normalized by the sample transmission at $B = 0$.

The samples were characterized in micro-Raman scattering experiments which, similarly to previous studies,²¹ revealed, depending on location, single-component 2D band features, characteristic of graphene simple electronic bands and of decoupled graphitic planes in multilayer epitaxial graphene grown on the C-face of a SiC substrate, or multi-component 2D band features characteristic of Bernal stacked graphite. In this paper, we present transmission data obtained on one particular specimen with a high number of graphitic layers (~ 100) and grown on a SiC substrate with a reduced thickness of ~ 100 μm . Due to this latter condition, the spectral region of total opacity of the sample only covers the SiC reststrahlenband (~ 85 -120 meV), i.e., it is significantly narrower as compared to the case of the preceding studies.^{28,29} In spite of these efforts to expand the available spectral range, a relatively weak transmission was still found around the energy of 200 meV, due to double-phonon absorptions in the underlying SiC substrate and transmission spectra are affected by strong interference patterns due to the relatively thin substrate. These two effects prevented measurements in the energy range below the reststrahlenband of SiC.

III. RESULTS AND DISCUSSION

Typical transmission spectra of the investigated sample are shown in Fig. 1. The dominant absorption lines which are observed in these spectra show the characteristic \sqrt{B} -dependence (see Fig. 2) and correspond to inter-LL transitions in electrically isolated graphene sheets.

We denote those lines by Roman letters, following the initial work and notation of Sadowski *et al.*^{13,28} These dominant spectral features are equivalent to the characteristic lines observed in the magneto-optical response of exfoliated graphene monolayers.^{14,15,18} The subsequent absorption lines labelled here as B \rightarrow I correspond to transitions $L_{-m(-m-1)} \rightarrow L_{m+1(m)}$ with $m = 0 \rightarrow 7$ between LLs in graphene: $E_m = \text{sign}(m)E_1\sqrt{|m|}$, where $E_1 = v_F\sqrt{2\hbar|eB|}$. The apparent Fermi velocity is extracted to be $v_F = (1.02 \pm 0.02) \times 10^6$ m.s⁻¹. Intriguingly, the $L_{-1(0)} \rightarrow L_{0(1)}$ transition exhibits a significant broadening above 16 T, which could be tentatively related to electron-phonon interaction. This effect will be discussed elsewhere.

The main focus of the present work are other spectral features, i.e., the transmission dips denoted by **n=1, n=2, ... n=5** in Fig. 1. These absorption lines are significantly weaker than the dominant “graphene lines”, but are still well resolved in our spectra. As it can be seen in Fig. 2, in contrast to the dominant transitions, these weaker lines follow a nearly linear in B dependence. As this behavior is characteristic of massive particles and because graphene bilayer is the simplest graphene based system with such particles, we anticipate that electronic excitations within graphene bilayer inclusions are responsible for the **n=1, n=2, ... n=5** transitions. The energy ladder $\varepsilon_{n,\mu}$ of LLs in a graphene bilayer can be easily calculated^{30,31} within the standard four band model which only considers the two most relevant coupling constants γ_0 and γ_1 (see e.g. Ref. 32 for their definitions):

$$\varepsilon_{n,\mu} = \text{sign}(n) \frac{1}{\sqrt{2}} \left[\gamma_1^2 + (2|n| + 1)E_1^2 + \mu \sqrt{\gamma_1^4 + 2(2|n| + 1)E_1^2\gamma_1^2 + E_1^4} \right]^{1/2}. \quad (1)$$

Here, a positive (negative) integer n indexes the electron (hole) LLs. $\mu = -1$ accounts for the topmost

valence- and the lowest conduction-band, whereas $\mu = 1$ corresponds to two other, split-off bands. As illustrated in the inset of Fig. 2, optically active inter Landau level transitions in a graphene bilayer fulfill the $|n| \rightarrow |n| \pm 1$ selection rule. The energies of such transitions are plotted in Fig. 2 with black solid lines. Those lines account for the transitions within the $\mu = -1$ bands. To reproduce the experimental data, we have adjusted the γ_1 parameter whereas the Fermi velocity v_F which defines E_1 (i.e. the intra-layer coupling $\gamma_0 = 3150$ meV) has been fixed at the value derived from the monolayer-like transitions. A fair agreement is obtained between the calculated (solid lines in Fig. 2) and measured energies of **n=1**, **n=2**, ... **n=5** transitions. Optical absorptions involving LLs of higher indexes (e.g. **n=6**, **n=7** and **n=8**, see Fig. 2) could also be observed in the spectra, nevertheless, these lines are very weak and only visible in a limited range of magnetic fields. Traces of inter-LL transitions due to split-off bands ($\mu = 1$ in Eq. 1), can be also identified in our data and experiments focused on this particular set of transitions are in progress.

A pronounced departure of the observed bilayer transitions from the linearity in B clearly shows the limits of the parabolic approximation which is often used for graphene bilayers in the close vicinity of the $\mathbf{k} = 0$ point, and within which the LLs are strictly linear with the magnetic field.^{32,33} As can be seen in Fig. 2, the positions of all these lines can be very well reproduced with a parameter $\gamma_1 = (385 \pm 5)$ meV, and these experiments thus refine the value of this parameter reported previously from optical studies at zero magnetic field.^{6,10,11} The intriguing splitting of the **n=1** and of the **n=2** lines at high magnetic fields is beyond our simple model and will be discussed later on.

The simplified model of LLs in the pristine bilayer graphene provides us with reasonably accurate description of its magneto-optical response, even though it neglects the electron-hole asymmetry (mainly induced by tight-binding γ_4 , Δ' parameters),^{6,8,10,11} as well as a possible gap opening at the charge neutrality point. Nevertheless, it should be noted that the optical response of the graphene bilayer has only been unambiguously identified above the reststrahlenband of the SiC substrate and therefore, we cannot exclude a possible appearance of an energy gap, up to a few tens of meV, at the $\mathbf{k} = 0$ point. For the same reason, we can only estimate a very higher limit for the carrier density in the studied bilayer of $2 \times 10^{12} \text{ cm}^{-2}$. However, the real carrier density is very likely similar to that of the surrounding (electrically isolated) graphene sheets, i.e. below 10^{10} cm^{-2} , as reported in Refs. 16 and 22. We also point out that relatively narrow linewidths of the order of 10 meV (relaxation time in sub-picosecond range) serve as an indication of rather high electronic quality of these bilayer inclusions, comparable or even better than other bilayer systems.^{12,34,35}

Equivalent bilayer-like spectral features are recurrently identified practically in all studied specimens, nevertheless, with a strongly varying intensity. In general, we

can say that the relative intensity of these “bilayer” lines increases with the total number of layers in MEG and these transitions are practically invisible in specimens with less than 10 layers reported in very first magneto-spectroscopy studies.^{13,28} This finding serves as an indication that we indeed observe graphene bilayer inclusions and not regions of a local AB-stacking which might be also speculated to appear in rotationally stacked multilayers. Such Moiré-patterned AB-stacked areas have been recently visualized in MEG by STM/STS measurements.³⁶⁻³⁸ We further assume that twisted graphene layers which results in the Moiré patterned bilayer should not provide us with so well-defined AB stacked bilayers as we observe in our data. Let us also note that if we compare the relative intensity of observed transitions, we can roughly estimate that in none of the investigated samples the ratio between bilayers and monolayers exceeded 10%.

We should also emphasize that the appearance of Bernal-stacked faults in MEG, which have a form of well-defined bilayers, is not a signature of bulk graphite. In this well known material, the K -point electrons indeed mimic massive carriers in the graphene bilayer, but with an effective inter-layer coupling $2\gamma_1$ instead of γ_1 in a real graphene bilayer.^{31,39-41} This twofold coupling in the effective bilayer model for K point electrons implies a characteristic effective mass twice enhanced in comparison to that of massive Dirac fermions in true graphene bilayer and consequently, also a twice lower energy separation between adjacent interband inter-LL transitions, cf. Fig. 2 of this paper with the fan chart in Ref. 40.

The remaining unclarified point of our study is the splitting of the bilayer lines, which is clearly visible for transitions **n=1** and **n=2** around $B = 17$ and 26 T, respectively. In the following, we discuss two different scenarios for this splitting. One possible explanation invokes the electron-hole asymmetry, reported recently in graphene bilayers graphene.^{6,10,11} Based on this assumption, the magnitude of the splitting for the n -th transition, relative to the transition energy is expressed by:⁴²

$$\frac{2(\Delta'/\gamma_1 + 2\gamma_4/\gamma_0)}{\sqrt{n(n+1)} + \sqrt{(n+1)(n+2)}}.$$

For the values $\Delta' = 0.02$ eV, $\gamma_1 = 0.4$ eV, $\gamma_4/\gamma_0 = 0.05$,^{6-8,10,11} our measured value for $n = 1$ (about 0.08) is very well reproduced. However, the splitting due to electron-hole asymmetry should be seen for all magnetic fields, while, as can be seen in Fig. 1b, we only observe it in a relatively narrow range of B .

Perhaps a more natural explanation for this line splitting would be an avoided crossing between the transition $L_{-n(-n-1)} \rightarrow L_{n+1(n)}$ and some other transition with a much smaller oscillator strength, so that it is not seen far from the crossing point. One can see directly from Fig. 2 that the bright transitions $n = 1, 2$ are crossed by the dark (i.e., dipole-inactive in case of a zero trigonal warping) transitions $L_{0(-4)} \rightarrow L_{4(0)}$, $L_{0(-7)} \rightarrow L_{7(0)}$, respectively, approximately at the observed values of B

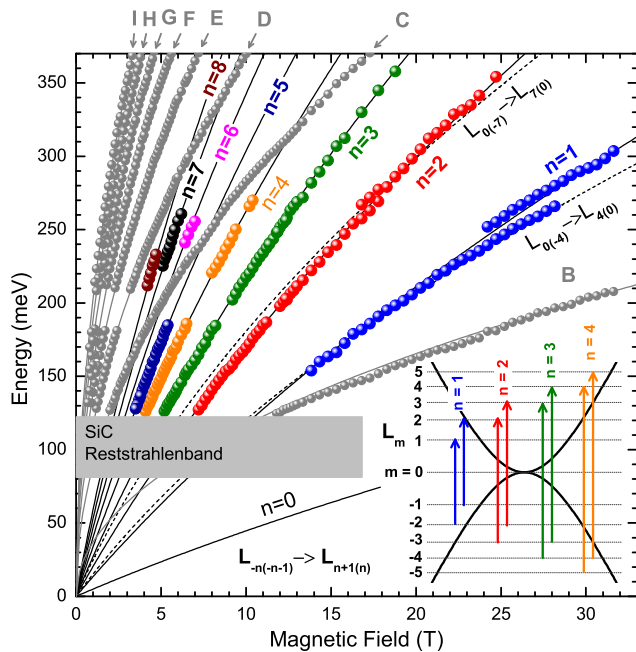


FIG. 2: (color online) Fan chart: Points marked with Roman letters, having a characteristic \sqrt{B} -dependence, correspond to inter-LL transitions in electrically isolated graphene sheets.¹³ Points denoted by index n represent inter-band inter-LL transitions in the graphene bilayer $L_{-n(-n-1)} \rightarrow L_{n+1(n)}$, as schematically shown in the inset. The full gray lines show expected energies of transitions in the graphene monolayer for $v_F = 1.02 \times 10^6 \text{ m.s}^{-1}$, full black lines correspond to predicted positions of the absorption lines in the graphene bilayer (only parameters $\gamma_0 = 3150 \text{ meV}$ and $\gamma_1 = 385 \text{ meV}$ considered). The dashed lines denote theoretical positions of two trigonal-warping-induced transitions in the graphene bilayer $L_{0(-4)} \rightarrow L_{4(0)}$ and $L_{0(-7)} \rightarrow L_{7(0)}$.

(the crossing occurs at a very sharp angle, which brings a significant uncertainty). These transitions are allowed only due to the presence of the trigonal warping of the electronic bands, which mixes levels L_m with $|m|$ differing by an integer multiple of 3, see Ref. 30. The ratio of the oscillator strength of the $L_{0(-4)} \rightarrow L_{4(0)}$ transition to that of the bright $n = 1$ transition can be estimated⁴² as $(25/108)(\gamma_3\gamma_1/\gamma_0)^2(l_B/\hbar v_F)^2 \simeq 0.02$ at $B = 25 \text{ T}$. The $L_{0(-4)} \rightarrow L_{4(0)}$ transition is therefore not expected to be seen in the experiment unless some other, possibly resonant, admixture mechanism is taken into account. Coupling between $L_{0(-4)} \rightarrow L_{4(0)}$ and $n = 1$ transitions should be quite strong as the observed “anti-crossing splitting” is of about 20 meV.

We have speculated this mode coupling could be due to electron-phonon or electron-electron interactions. Electron-phonon interaction, which could be enhanced due to the proximity of the transition energy (250 meV) to that of the zone-center optical phonon (196 meV), must be excluded due to the different symmetry (this phonon is Raman active). Splitting due to Coulomb interaction can be evaluated to be $0.04(e^2/4\pi\epsilon_0\hbar v_F)(\gamma_1\gamma_3/\gamma_0)$,⁴² i.e. only about 3 meV in the absence of dielectric screening, $e^2/4\pi\epsilon_0\hbar v_F = 2.2$. Hence, the mechanism of the possible strong coupling between the $L_{-1(-2)} \rightarrow L_{2(1)}$ and $L_{0(-4)} \rightarrow L_{4(0)}$ transitions is a puzzle which remains to be clarified.

IV. CONCLUSIONS

We probed graphene bilayers embedded in multilayer epitaxial graphene on the C-terminated surface of SiC. These inclusions can be viewed as AB-stacked faults in an otherwise rotationally-stacked multilayer graphene structure and enable spectroscopic studies of unperturbed graphene bilayers. The “electronic quality” of these bilayers is comparable or even better than that of the bilayers obtained by exfoliation or by epitaxial growth on the Si-terminated surface of SiC.^{34,35} This way, we could trace the inter-band inter-LL transitions in the graphene bilayer for the first time, and thus supply data complementary to the cyclotron resonance absorption (i.e., intra-band inter-LL transitions) measured on the exfoliated bilayer by Henriksen *et al.*¹² We could also clearly visualize the departure of Landau levels in the graphene bilayer from the linearity in B , which clearly sets limits for the parabolic approximation of electronic bands in this material.

Acknowledgments

We acknowledge also funding received from EC-EuroMagNetII under Contract No. 228043, from the Keck Foundation and from the Partner University Fund at the Embassy of France. This work has been supported by the Projects No. 395/NPICS-FR/2009/0, No. MSM0021620834, GACR No. P204/10/1020 and No. MTKD-CT-2005-029671, furthermore by Grants No. 670/N-ESF-EPI/2010/0, No. 671/NESF-EPI/2010/0, and No. GRA/10/E006 within the ESF EuroGraphene programme (EPIGRAT).

* Electronic address: milan.orldita@lncmi.cnrs.fr; also at Institute of Physics, v.v.i., ASCR, Prague, Czech Republic

¹ K. S. Novoselov, Nature Mater. **6**, 720 (2007).

² J. Bai, X. Zhong, S. Jiang, Y. Huang, and X. Duan, Nature

Nanotechnology **5**, 190 (2010).

³ S. Y. Zhou, G.-H. Gweon, A. V. Fedorov, P. N. First, W. A. de Heer, D.-H. Lee, F. Guinea, A. H. C. Neto, and A. Lanzara, Nature Mater. **6**, 770 (2007).

- ⁴ A. Bostwick, T. Ohta, T. Seyller, K. Horn, and E. Rotenberg, *Nature Phys.* **3**, 36 (2007).
- ⁵ R. Balog, B. Jorgensen, L. Nilsson, M. Andersen, E. Rienks, M. Bianchi, M. Fanetti, E. Lagsgaard, A. Baraldi, S. Lizzit, et al., *Nature Materials* **9**, 315 (2010).
- ⁶ A. B. Kuzmenko, E. van Heumen, D. van der Marel, P. Lerch, P. Blake, K. S. Novoselov, and A. K. Geim, *Phys. Rev. B* **79**, 115441 (2009).
- ⁷ K. F. Mak, C. H. Lui, J. Shan, and T. F. Heinz, *Phys. Rev. Lett.* **102**, 256405 (2009).
- ⁸ Y. Zhang, T.-T. Tang, C. Girit, Z. Hao, M. C. Martin, A. Zettl, M. F. Crommie, Y. R. Shen, and F. Wang, *Nature* **459**, 820 (2009).
- ⁹ M. F. Craciun, S. Russo, M. Yamamoto, J. B. Oostinga, A. F. Morpurgo, and S. Tarucha, *Nature Nanotech.* **4**, 383 (2009).
- ¹⁰ L. M. Zhang, Z. Q. Li, D. N. Basov, M. M. Fogler, Z. Hao, and M. C. Martin, *Phys. Rev. B* **78**, 235408 (2008).
- ¹¹ Z. Q. Li, E. A. Henriksen, Z. Jiang, Z. Hao, M. C. Martin, P. Kim, H. L. Stormer, and D. N. Basov, *Phys. Rev. Lett.* **102**, 037403 (2009).
- ¹² E. A. Henriksen, Z. Jiang, L.-C. Tung, M. E. Schwartz, M. Takita, Y.-J. Wang, P. Kim, and H. L. Stormer, *Phys. Rev. Lett.* **100**, 087403 (2008).
- ¹³ M. L. Sadowski, G. Martinez, M. Potemski, C. Berger, and W. A. de Heer, *Phys. Rev. Lett.* **97**, 266405 (2006).
- ¹⁴ Z. Jiang, E. A. Henriksen, L. C. Tung, Y.-J. Wang, M. E. Schwartz, M. Y. Han, P. Kim, and H. L. Stormer, *Phys. Rev. Lett.* **98**, 197403 (2007).
- ¹⁵ R. S. Deacon, K.-C. Chuang, R. J. Nicholas, K. S. Novoselov, and A. K. Geim, *Phys. Rev. B* **76**, 081406R (2007).
- ¹⁶ M. Orlita, C. Faugeras, P. Plochocka, P. Neugebauer, G. Martinez, D. K. Maude, A.-L. Barra, M. Sprinkle, C. Berger, W. A. de Heer, et al., *Phys. Rev. Lett.* **101**, 267601 (2008).
- ¹⁷ P. Neugebauer, M. Orlita, C. Faugeras, A.-L. Barra, and M. Potemski, *Phys. Rev. Lett.* **103**, 136403 (2009).
- ¹⁸ E. A. Henriksen, P. Cadden-Zimansky, Z. Jiang, Z. Q. Li, L.-C. Tung, M. E. Schwartz, M. Takita, Y.-J. Wang, P. Kim, and H. L. Stormer, *Phys. Rev. Lett.* **104**, 067404 (2010).
- ¹⁹ I. Crassee, J. Levallois, A. L. Walter, M. Ostler, A. Bostwick, E. Rotenberg, T. Seyller, D. van der Marel, and A. B. Kuzmenko, arXiv:1007.5286 (2010).
- ²⁰ M. Mucha-Kruczynski, E. McCann, and V. Fal'ko, *Solid State Commun.* **149**, 1111 (2009).
- ²¹ C. Faugeras, A. Nerrière, M. Potemski, A. Mahmood, E. Dujardin, C. Berger, and W. A. de Heer, *Appl. Phys. Lett.* **92**, 011914 (2008).
- ²² M. Sprinkle, D. Siegel, Y. Hu, J. Hicks, A. Tejada, A. Taleb-Ibrahimi, P. L. Fevre, F. Bertran, S. Vizzini, H. Enriquez, et al., *Phys. Rev. Lett.* **103**, 226803 (2009).
- ²³ M. Sprinkle, J. Hicks, A. Tejada, A. Taleb-Ibrahimi, P. L. Fevre, F. Bertran, H. Tinkey, M. Clark, P. Soukiassian, D. Martinotti, et al., arXiv:1001.3869 (2010).
- ²⁴ D. A. Siegel, C. G. Hwang, A. V. Fedorov, and A. Lanzara, *Phys. Rev. B* **81**, 241417 (2010).
- ²⁵ C. Berger, Z. Song, T. Li, X. Li, A. Y. Ogbazghi, R. Feng, Z. Dai, A. N. Marchenkov, E. H. Conrad, P. N. First, et al., *J. Phys. Chem. B* **108**, 19912 (2004).
- ²⁶ J. Hass, F. Varchon, J. E. Millán-Otoya, M. Sprinkle, N. Sharma, W. A. de Heer, C. Berger, P. N. First, L. Magaud, and E. H. Conrad, *Phys. Rev. Lett.* **100**, 125504 (2008).
- ²⁷ D. L. Miller, K. D. Kubista, G. M. Rutter, M. Ruan, W. A. de Heer, P. N. First, and J. A. Stroscio, *Science* **324**, 924 (2009).
- ²⁸ M. L. Sadowski, G. Martinez, M. Potemski, C. Berger, and W. A. de Heer, *Solid State Commun.* **143**, 123 (2007).
- ²⁹ P. Plochocka, C. Faugeras, M. Orlita, M. L. Sadowski, G. Martinez, M. Potemski, M. O. Goerbig, J.-N. Fuchs, C. Berger, and W. A. de Heer, *Phys. Rev. Lett.* **100**, 087401 (2008).
- ³⁰ D. S. L. Abergel and V. I. Fal'ko, *Phys. Rev. B* **75**, 155430 (2007).
- ³¹ M. Koshino and T. Ando, *Phys. Rev. B* **77**, 115313 (2008).
- ³² E. McCann and V. I. Fal'ko, *Phys. Rev. Lett.* **96**, 086805 (2006).
- ³³ K. S. Novoselov, E. McCann, S. V. Morozov, V. I. Fal'ko, K. I. Katsnelson, U. Zeitler, D. Jiang, F. Schedin, and A. K. Geim, *Nature Phys.* **2**, 177 (2006).
- ³⁴ T. Ohta, A. Bostwick, T. Seyller, K. Horn, and E. Rotenberg, *Science* **313**, 951 (2006).
- ³⁵ C. Riedl, C. Coletti, T. Iwasaki, A. A. Zakharov, and U. Starke, *Phys. Rev. Lett.* **103**, 246804 (2009).
- ³⁶ D. L. Miller, K. D. Kubista, G. M. Rutter, M. Ruan, W. A. de Heer, P. N. First, and J. A. Stroscio, *Phys. Rev. B* **81**, 125427 (2010).
- ³⁷ D. L. Miller, K. D. Kubista, G. M. Rutter, M. Ruan, W. A. de Heer, M. Kindermann, P. N. First, and J. A. Stroscio, *Nature Phys.* p. to be published (2010).
- ³⁸ M. Kindermann and P. N. First, arXiv:1009.4492 (2010).
- ³⁹ B. Partoens and F. M. Peeters, *Phys. Rev. B* **75**, 193402 (2007).
- ⁴⁰ M. Orlita, C. Faugeras, J. M. Schneider, G. Martinez, D. K. Maude, and M. Potemski, *Phys. Rev. Lett.* **102**, 166401 (2009).
- ⁴¹ K.-C. Chuang, A. M. R. Baker, and R. J. Nicholas, *Phys. Rev. B* **80**, 161410(R) (2009).
- ⁴² This expression is obtained in the two-band approximation. The degree of error introduced by this approximation at energies about 250 meV can be roughly estimated from the deviation of the curves in Fig. 2 from their low-field tangents, which gives about 30%.